

Article

Phytic Acid-Silica System for Imparting Fire Retardancy in Wood Composites

Chia-Feng Lin ^{1,*}, Chi Zhang ¹, Olov Karlsson ¹, Jozef Martinka ², George I. Mantanis ^{3,*}, Peter Rantuch ², Dennis Jones ^{1,4} and Dick Sandberg ^{1,4}

- ¹ Wood Science and Engineering, Department of Engineering Sciences and Mathematics, Luleå University of Technology, SE-931 77 Skellefteå, Sweden; chizha-9@student.ltu.se (C.Z.); dennis.jones@ltu.se (D.J.); dick.sandberg@ltu.se (D.S.)
- ² Faculty of Materials Science and Technology in Trnava, Slovak University of Technology in Bratislava, Jana Bottu 2781/25, SK-917 24 Trnava, Slovakia; jozef.martinka@stuba.sk (J.M.); peter.rantuch@stuba.sk (P.R.)
- ³ Laboratory of Wood Science and Technology, Faculty of Forestry, Wood Sciences and Design, University of Thessaly, GR-431 00 Karditsa, Greece
- ⁴ Department of Wood Processing and Biomaterials, Faculty of Forestry and Wood Sciences, Czech University of Life Sciences Prague, Praha 6, CZ-16521 Prague, Czech Republic
- * Correspondence: chia-feng.lin@ltu.se (C.-F.L.); mantanis@uth.gr (G.I.M.); Tel.: +46-910-585308 (C.-F.L.)

Abstract: Fire-retardant (FR) treated wood-based panels, used commonly in furniture and construction, need to meet stringent fire safety regulations. This study presents a novel treatment for imparting fire resistance to wood composites by applying separate solutions of phytic acid and sodium silicate onto wood particles before the hot pressing at 160 °C. A scanning electron microscopy-energy dispersive X-ray spectroscopy (SEM-EDX) analysis revealed that phytic acid and sodium silicate were uniformly distributed throughout the wood particles, and the formation of silica gel resulted in the aggregation of elemental silicon. Fourier-transform infrared spectroscopy (FTIR) displayed that phytic acid caused the thermal degradation of hemicelluloses, which led to a brownish outer appearance of the FR-treated composites. Fire performance was assessed using both limiting oxygen index (LOI) and a cone calorimeter. These techniques showed a higher LOI value and a significant reduction in heat-release rate (HRR), total heat release (THR), smoke-production rate (SPR), and total smoke production (TSP). In addition, cone calorimeter and thermogravimetric (TGA) analyses consistently showed increased char residue in treated wood composites. Moreover, internal bond strength (IB) and modulus of elasticity (MOE) of the wood composite were not significantly changed compared with those of the untreated composite. Surprisingly, in the FR-treated composite, the 24 h-thickness swelling, and the water uptake were slightly decreased. Consequently, this new treatment has the potential to increase the fire retardancy of wood composites, such as particleboard, without deteriorating the key mechanical properties.

Keywords: inorganic-organic hybrid system; sodium phytate; fire retardant; particleboard



Citation: Lin, C.-F.; Zhang, C.; Karlsson, O.; Martinka, J.; Mantanis, G.I.; Rantuch, P.; Jones, D.; Sandberg, D. Phytic Acid-Silica System for Imparting Fire Retardancy in Wood Composites. *Forests* **2023**, *14*, 1021. <https://doi.org/10.3390/f14051021>

Academic Editor: Mathieu Petrisans

Received: 21 April 2023

Revised: 10 May 2023

Accepted: 11 May 2023

Published: 16 May 2023



Copyright: © 2023 by the authors. Licensee MDPI, Basel, Switzerland. This article is an open access article distributed under the terms and conditions of the Creative Commons Attribution (CC BY) license (<https://creativecommons.org/licenses/by/4.0/>).

1. Introduction

Wood-based panels such as particleboard, fibreboard, oriented strand board (OSB), and plywood are very common products for furniture and construction applications [1]. These panels are typically produced by bonding wood particles, fibres, strands, or veneers, by using water-borne, formaldehyde-based adhesives such as urea-formaldehyde (UF), melamine-urea-formaldehyde (MUF), or phenol-formaldehyde (PF) prepolymers under high pressure and heat [2]. However, due to the inherently low fire resistance of wood, fire retardant additives (FRs) are incorporated into the panels for use in public buildings where fire safety is of paramount importance [3]. Conventional FRs such as, for instance, ammonium phosphate salts, for instance, ammonium dihydrogen phosphate, ammonium polyphosphates (APP), and urea phosphate, among others, have been used in the industry

to increase the fire retardancy of wood-based panels [4,5]. These FRs are well-known for their affordability, effectiveness, and low toxicity. Phosphate-containing compounds are particularly effective in advancing the fire resistance of wooden materials. This is due to their ability to promote the formation of char in the OH-abundant polymers and to condense as a polyphosphate to protect the inner part of the material from catching fire. In addition, they act as radical scavengers by terminating the combustion. Moreover, the ammonium component has a synergetic action with phosphate-containing compounds, as they are decomposed into N_2 or NH_3 to reduce the contact with the combustible gas O_2 .

Recently, phytic acid ($C_6H_{18}O_{24}P_6$), a six-fold dihydrogen phosphate ester of inositol, was explored for its prospective to upgrade the fire retardancy of lignocellulosic materials [6–11]. This phosphate-rich compound is mainly sourced from nuts, oilseeds, and cereals, and it is comprised of six phosphate groups attached to a six-carbon ring, unlike conventional phosphates obtained from minerals. However, due to its high acidity, it can cause deterioration in the mechanical properties of materials at elevated processing temperatures. To address this issue, the reaction of phytic acid with urea was suggested in order to form ammonium phytate, which reduces the acidity and provides a synergistic fire retardancy [11,12]. While ammonium phosphate-based fire retardants have been proved to substantially decrease heat release, they possess limited efficacy in suppressing smoke production. To overcome this limitation, inorganic compounds such as $CuSO_4$, $FeSO_4$, $MgSO_4$, $ZnSO_4$, SiO_2 , $Al(OH)_3$, and zinc borate have been proposed in combination with phytic acid-based FRs [5,13–15]. This combined approach has been shown to further suppress smoke production and enhance fire retardancy in wood-based materials. For example, the combination of nano- SiO_2 with phytic acid has been shown to have a smoke suppression effect on solid wood [15].

Inorganic silica (SiO_2) is commonly synthesised from a sodium silicate (Na_2SiO_3 , water glass) precursor solution through the sol-gel method, which requires an acid (e.g., H_2SO_4 or $Al_2(SO_4)_3$) [16,17]. The reduction in pH causes the formation of silicic acid, which further condenses/polymerizes as a solid SiO_2 gel. The size of the SiO_2 gel particle can be controlled by varying the temperature, pH, and other parameters (e.g., particle concentration, particle charge, and surface tension) of the precursor solution [16,18]. The incorporation of SiO_2 into wood has been utilized for protection against ultraviolet (UV) light and fire [19–22]. This is achieved by impregnating the wood structure with sodium silicate solution, followed by drying. The deposition of SiO_2 in the wood matrix relies upon the reaction of sodium silicate with carbonic acid (CO_2 from air dissolved in water) to initiate the sol-gel process. However, using sodium silicate for treating wood comes with some disadvantages. The high alkali solution can potentially cause mechanical property deterioration at elevated temperatures, a fact that makes the modification of solid wood with sodium silicate a highly complicated approach [19]. Furthermore, the high viscosity of the various solutions may limit the penetration depth. However, in the wood-panel production process, it may be easier to incorporate the sodium silicate solution. In fact, spraying sodium silicate solution onto wood particles as a pre-treatment can be easily realised.

Herein, a new approach for upgrading the fire retardancy of wood composites is proposed. This process involves pre-treating wood particles by sequentially spraying them with aqueous solutions of phytic acid and sodium silicate. The acidic phytic acid acts as a catalyst for the sodium silicate to form thermally stable silica gels. The sodium ions from the sodium silicate and phytic acid are combined to form sodium phytate, which is expected to provide synergistic fire retarding properties by improving the smoke suppression of the system. This process also neutralizes the highly acidic phytic acid and the highly alkaline sodium silicate, which alleviates the detrimental effects on the adhesive curing during the hot-pressing. The chemical functionalities of the inorganic-organic hybrid wood composites produced in this work were examined by Fourier transform infrared spectroscopy (FTIR). The elemental distribution was carried out by using scanning electron microscopy–energy dispersive X-ray analysis (SEM-EDX). Additionally, the thermal behaviour was investigated by thermogravimetric analysis (TGA), while the fire performance was examined by

2.3. Characterization

The infrared spectra were recorded using a PerkinElmer FTIR Frontier spectrometer (Waltham, MA, USA) equipped with a UATR Diamond/ZnSe ATR (single reflection). The surface of the specimens was collected using a knife before being analysed over the wavenumber range of 4000–650 cm^{-1} with four scans at a resolution of 4 cm^{-1} . Three replicates were used. The pH of the wood composites was measured by a Metrohm pH meter 744 (Herisau, Switzerland). This value was determined by soaking 0.15 g of wood composites powder in 6 g of DI water. Scanning electron microscopy–energy dispersive X-ray (SEM-EDX, JeolJSM-IT300LV, Tokyo, Japan) was used to analyse the morphology and the elemental distribution of the specimens under low-vacuum mode at 100 Pa through secondary electron (SE) mode. The acceleration voltage of the electron beam was set at 10 kV for the SEM, and 15 kV for EDX, respectively. The spectrometer was operated using Oxford Instruments ZAtec V3.1 software (Buckinghamshire, UK). A surface sample of the specimen was collected using a knife and placed on conductive carbon tape without coating. Scanning times of about 300 sec were used for the EDX mapping. A thermogravimetric analysis (TGA) was carried out using a PerkinElmer TGA 4000 (Waltham, MA, USA). About 5 mg of specimen was collected with a knife and loaded in an alumina crucible before being heated from 30 °C to 800 °C at a constant heat rate of 10 °C min^{-1} under a purge gas N_2 at a flow rate of 20 mL min^{-1} . The first-order derivative curve of the TGA (DTG curve) was smoothed using a 20-point smooth algorithm through Mettler Toledo STARe Evaluation software V16.20. A limiting oxygen index (LOI, Fire Testing Technology Ltd., East Grinstead, UK) was performed (according to the ISO 4589 standard) [23] on five replicates with dimensions of 10 × 10 × 150 mm. The cone calorimeter test was performed by following the ISO 5660-1 standard [24] under a heat flux of 50 kW/m^2 on five replicates with dimensions of 100 × 10 × 100 mm. The modulus of elasticity (MOE) and modulus of rupture (MOR) were determined on five specimens with dimensions of 180 × 10 × 10 mm through the use of a by four-point bending test described in the EN 408 standard [25] using an MTS Systems Corporation Criterion Model 43 universal testing machine (Créteil, France). The internal bond strength (IB) was determined according to the EN319 standard [26]. The thickness swelling of the specimens after 2 h and 24 h of soaking in distilled water was determined according to the EN317 standard [27]. The water uptake during the thickness swelling test was also evaluated.

3. Results and Discussion

3.1. Chemical Functionalities, Appearance, and Elemental Distribution

The chemical functionalities of the specimens analyzed by FTIR, are presented in Figure 2a. The spectrum of the untreated wood is attributed to the wood polymeric constituents of cellulose, hemicelluloses, and lignin [28]. After spraying the MUF adhesive and following the hot-pressing, the produced wood composite (‘unmodified’) revealed the band shifting from 1738 cm^{-1} to 1727 cm^{-1} , which is due to the autocatalytic thermal degradation of principal hemicellulose, galactoglucomannan, during the hot-pressing, by cleaving the O–acetyl bond with the formation of acetic acid [29]. The band originally at 808 cm^{-1} , corresponding to the C–H out-of-plane bending in lignin, was shifted to the band at 812 cm^{-1} . This shift was due to the overlapping with the band attributed to the triazole rings from the melamine of the MUF adhesive [28,30].

The introduction of FRs changed the chemical functionalities of the wood composites. The band originally located at 1727 cm^{-1} of the unmodified wood composite was further shifted to the lower band at 1722 cm^{-1} along with the increasing concentration of the FR additives. This is probably related to the acidity of the phytic acid acting as a catalyst, promoting the thermal degradation of hemicelluloses by cleaving the O–acetyl bonds [8,9]. This is supported by the pH values of the unmodified, 6-FR, 9-FR, and 12-FR wood composites, which measured 4.84, 2.95, 2.75, and 2.72, respectively. Additionally, the protonation of acetic acid could also lead to the band shifting. The thermal degradation can also cause the brownish colour of the treated specimens, as shown in Figure 2b. The

band at 1657 cm^{-1} assigned to the conjugated C=O stretching was shifted to a lower band and was more pronounced at 1638 cm^{-1} . This is likely attributed to peak overlapping with the vibration stretching of O–P–O from phytic acid at 1638 cm^{-1} [31]. The band at about 1000 cm^{-1} is related to the vibration stretching of the ether bond C–O–C of the wood components cellulose, hemicelluloses, and lignin, which is overlapped with the Si–O–Si network of SiO_2 from sodium silicate [32]. The band at 812 cm^{-1} contributed to the MUF adhesive [28]. Finally, the other bands of the FR-modified wood composite are similar to those of the unmodified wood composite.

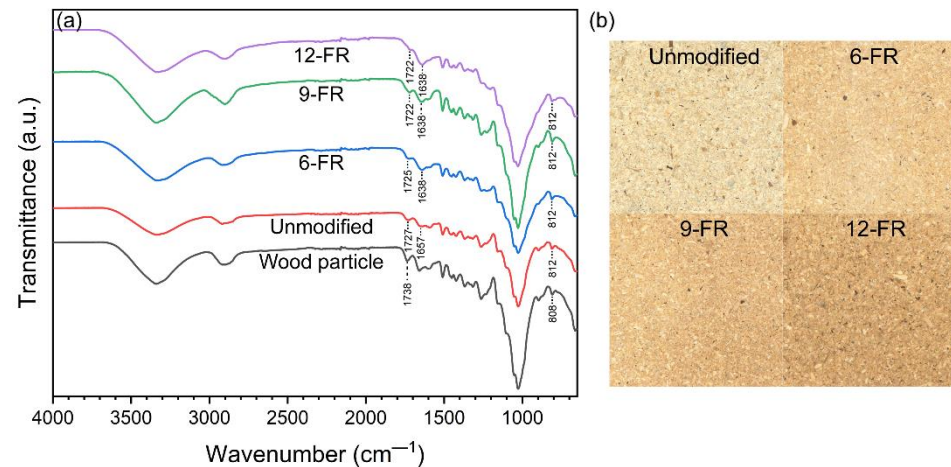


Figure 2. Chemical functionalities and appearance of the wood composites: (a) FTIR spectra and (b) appearance of the unmodified, 6-FR, 9-FR, and 12-FR wood composites.

The SEM-EDX analysis of the 12-FR specimens is presented in Figure 3a–h. The SEM image in Figure 3a revealed a much less porous anatomical appearance of the wood, as seen in the lumina, pits, bordered pits, and resin canals, due to the compression of the wood particles during hot-pressing. The mechanical grinding for making wood particles could also lead to damage in the particles, resulting in fewer anatomical features. Moreover, the filling of the MUF adhesive to the porous structure of wood may have contributed to the smoother surface [33].

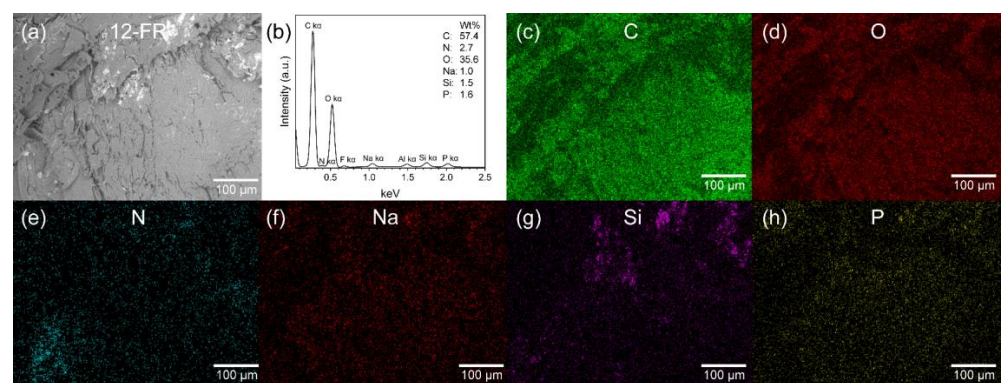


Figure 3. SEM-EDX analysis: (a) SEM image (b) EDX spectrum, and (c–h) the elemental mapping of elemental C, O, N, Na, Si, and P, respectively. The 12-FR wood composite was used for this investigation.

The EDX spectrum of the SEM image in Figure 3b shows the main composition of the 12-FR specimen, including C, N, O, F, Na, Al, Si, and P. The presence of elemental Al is due to the sample holder, while the presence of elemental F is a result of the microtome blade contamination during the sample preparation. The elemental C and O are mainly

derived from cellulose, hemicelluloses, and lignin, as well as from the MUF resin and phytic acid [28]. The elemental N is mainly attributed to the nitrogenous components of the MUF adhesive, such as urea and melamine. The elemental P is attributed to the phytic acid. The elemental Na and Si mostly originated from the sodium silicate.

Characteristically, the weight ratio of Na:Si over the mapping image in the EDX spectra was 0.67, which is close to the theoretical value of the sodium silicate applied (0.69). It was unusual to note an uneven distribution of elemental Si by EDX mapping, which shows as white spots in the SEM image and elemental Si mapping (Figure 3g). This segregation is likely the result of the condensation of the silica gel [20].

These findings suggest that the aqueous solutions of sodium silicate, phytic acid, and MUF adhesive were evenly sprayed during the FR wood composite manufacturing, while the formation of silica gelled to a higher contrast in specific areas of the SEM image.

3.2. Thermal Behaviour

The thermal behaviour of the wood composites produced with different concentrations of FR additives determined by TGA is presented in Figure 4. The unmodified wood composite exhibited three stages of thermal degradation. The first stage, beginning at 30 °C and ending at around 120 °C, is related to the removal of the bound water. The following stage, between 250 °C and 420 °C, with a maximum decomposition temperature at 364 °C, is related to the thermal decomposition of wood components, namely hemicelluloses and cellulose [28]. At this stage, volatile degradation products such as levoglucosan, furfural, acetic acid, CO₂, CO, and H₂O are produced [34,35]. The main thermal decomposition of MUF adhesive also occurs at this stage, involving the cleavage of side groups in the MUF polymeric network, with the release of small molecules such as CO₂, NH₃, methanol, formaldehyde, and amines [36,37]. Temperatures above 420 °C, up to approximately 700 °C, are related to the thermal decomposition of the most thermally stable constituent, which is lignin, as well as to the decomposition of the condensed cyameluric (i.e., heptazine) structures of the MUF adhesive [28,38]. The mass residue of the unmodified wood composite at 800 °C is approximately 2.6 wt% of its initial mass.

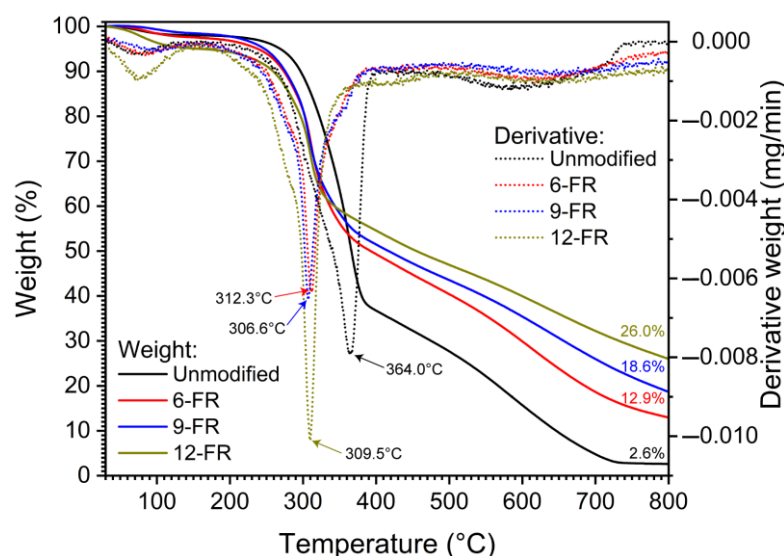


Figure 4. TGA and DTG curves of the unmodified 6-FR, 9-FR, and 12-FR wood composites.

The addition of FRs in the wood structure had a significant impact on the thermal behaviour of the composites, as evidenced by the lower main decomposition temperature and the increase in residue. For all FR wood composites, the main decomposition temperature was evidently shifted to a lower temperature of around 310 °C. This is mainly due to the influence of phytic acid with the promotion of dense char at a lower temperature to prevent further thermal degradation of the material [8,9]. Furthermore, the condensation

of phosphate groups led to the formation of polyphosphate, which acts as a protective insulation layer [39]. Silica gel is supposed to act as an incombustible inert material, thereby increasing the final char residue [40]. As the concentration of FRs increases, the amount of residue at 800 °C also increases. Noticeably, the 12-FR specimen exhibited the highest char residue, at 26% of its initial mass at 800 °C.

3.3. Fire Performance

The fire performance of the wood composite examined by the limiting oxygen index (LOI) is presented in Figure 5a. A higher LOI value indicates a higher level of O₂ concentration required to sustain combustion, which simply suggests a higher fire resistance [5]. The result showed that the 12-FR wood composite had the highest LOI value, which corresponded to the highest amount of FR added to the specimen.

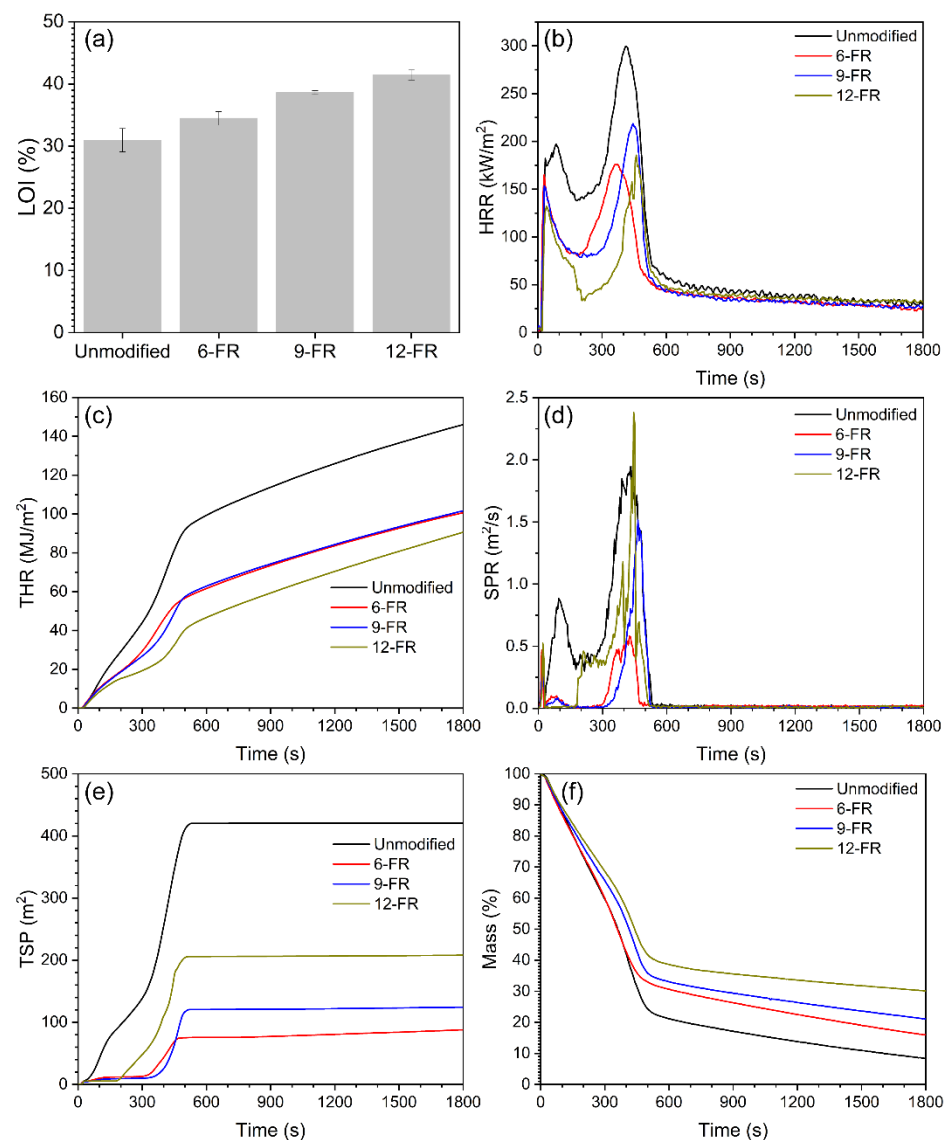


Figure 5. Fire performance according to (a) limiting oxygen index (LOI), and (b–f) the cone calorimeter results of the heat release rate (HRR), total heat release (THR), smoke-production rate (SPR), total smoke production (TSP), and mass loss of the unmodified, 6-FR, 9-FR, and 12-FR wood composites produced, respectively.

The fire performance of the wood composite was further evaluated using a cone calorimeter in order to analyse its heat and smoke release behaviour, as depicted in

Figure 5b–f and Table 1. It is worthy of note that the heat-release rate (HRR) is the most critical parameter for identifying the fire retarding properties of a material. The unmodified wood composite exhibited typical heat-release behaviour, with two HRR peaks, as shown in Figure 5b. The first peak occurs during surface oxidation, releasing heat, while the valley before the second peak results from surface charring. The second peak is a result of the overheating of the specimen in its entire thickness, which is typical for thermally thick materials placed on an insulating material [41]. The subsequent reduction of HRR arises out of the glowing of the char after consuming volatile products [28,42].

Table 1. Time to ignition (TTI), first peak of heat release rate (pHRR₁), second peak of heat release rate (pHRR₂), total heat release (THR), maximum average rate of heat emission (MARHE), effective heat of combustion (EHC), total smoke production (TSP), residue mass, and time to flashover values for the unmodified, 6-FR, 9-FR, and 12-FR wood composites. The values in parentheses are the standard deviations.

Specimen	Unmodified	6-FR	9-FR	12-FR
TTI (s)	24 (2)	19 (3)	21 (4)	25 (2)
pHRR ₁ (kW/m ²)	200 (12)	168 (14)	157 (4)	135 (2)
pHRR ₂ (kW/m ²)	314 (17)	193 (26)	222 (11)	203 (35)
THR (MJ/m ²)	146 (11)	101 (14)	102 (5)	91 (6)
TSP (m ²)	421 (44)	88 (23)	124 (15)	208 (169)
Residue mass (%)	8.39 (1.03)	15.95 (1.47)	21.10 (1.25)	30.11 (4.55)
EHC (MJ/kg)	15.03 (0.98)	12.48 (1.62)	12.17 (0.43)	11.19 (1.03)
MARHE (kW/m ²)	185 (7)	118 (6)	116 (1)	91 (8)
Time to flashover (s)	433 (41)	566 (85)	740 (133)	1616 (648)

The addition of FRs substantially reduced the heat release of the wood composites, resulting in lower peaks of HRR and total heat release (THR). The phosphate group from the phytic acid is particularly effective in reducing the heat release of lignocellulosic materials, since it acts as a radical scavenger, promotes char residue, and forms protective insulation layers. During combustion, the production of P radicals can scavenge the O and H radicals that are produced, thus terminating the combustion behaviour. Protons from phytic acid can accelerate the dehydration of the hydroxyl groups from wood particles and promote char residue. Simultaneously, the release of water molecules causes a decrease of concentration, or partial pressure, of oxygen in the combustion zone. The dehydration of phosphate with the formation of polyphosphate can create protective glassy layers that prevent further combustion. Silica gel acts as a physical barrier, suppressing smouldering and flaming combustion by preventing flammable products from escaping and preventing the matrix from contacting the O₂ [39].

Regarding the smoke production, Figure 5d,e shows that the FRs can greatly suppress the smoke production. However, it should be noted that the total smoke production (TSP) increased proportionally to the concentration of FRs, primarily due to the limited smoke suppression ability of phosphate-based fire retardants such as phytic acid on lignocellulosic materials [5,43]. To achieve better smoke suppression, a combination with inorganic compounds, such as the synergetic effect of phytic acid and sodium ions, is suggested, which has been shown to be more efficient than phytic acid alone [44]. This result implies that the amount of sodium silicate can be further increased for better smoke suppression. Additionally, based on the results of FTIR and the brown colour of the FR wood composites, the FR wood composites were rather more acidic than the unmodified specimen during the hot-pressing. This result actually confirms the potential of increasing the amount of alkaline sodium silicate for the optimization of smoke suppression. However, it is important to consider the influence of pH on the hardening of the MUF adhesive. The mass residue of the specimens was found to be proportional to the amount of FR additives; this alone confirms the promotion of char residue, as observed in the TGA analysis.

Furthermore, Table 1 includes the results of other key fire performance parameters, such as time to ignition (TTI), effective heat of combustion (EHC), maximum average rate of heat emission (MARHE), and prediction of time to flashover. The TTI measures the time required for the material to ignite. This FR treatment had a negligible effect on TTI, possibly due to the similar density between the groups [45]. The EHC represents the amount of heat released per unit mass of material burned. The MARHE is a single value estimation of the fire performance originally defined in the EN 45545-2 standard [46,47] for comparing the fire hazard of different materials. A lower value of MARHE indicates a lower fire hazard. The prediction of time to flashover estimates the early stages of a fire from the ignition source up to the flashover [48], and this calculation is based on the THR and TTI of the cone calorimeter by the method developed by [49]. A higher value means a lower fire growth hazard of the material. The improvement in these values of the FR wood composites suggests that the treatment effectively enhances the fire retardancy. Overall, the LOI and cone calorimeter results support the conclusion that the fire retarding properties of wood composites were significantly enhanced by combining the phytic acid and sodium silicate as FRs. The mechanism of phytic acid and sodium silicate treatment can be concluded as involving char formation, the creation of inert layers by polyphosphate and silica gel, and radical scavenging. Additionally, the smoke production was suppressed, which is likely related to the use of sodium silicate.

3.4. Mechanical and Physical Properties

The impact of FRs on the mechanical and physical properties of the treated wood composite, was assessed through the four-point bending test, internal bond strength (IB), water uptake, and thickness swelling. The results are presented in Figure 6. The MOE and MOR (Figure 6a,b indicates that the FRs do not significantly influence the MOE, while the MOR seemed to be slightly reduced. The MOR is determined by the maximum load that the material can withstand before fracture. The reduction of MOR might be due to the extensive thermal degradation of the hemicelluloses caused by phytic acid during hot-pressing [50], thus affirming the observation of the FTIR analysis.

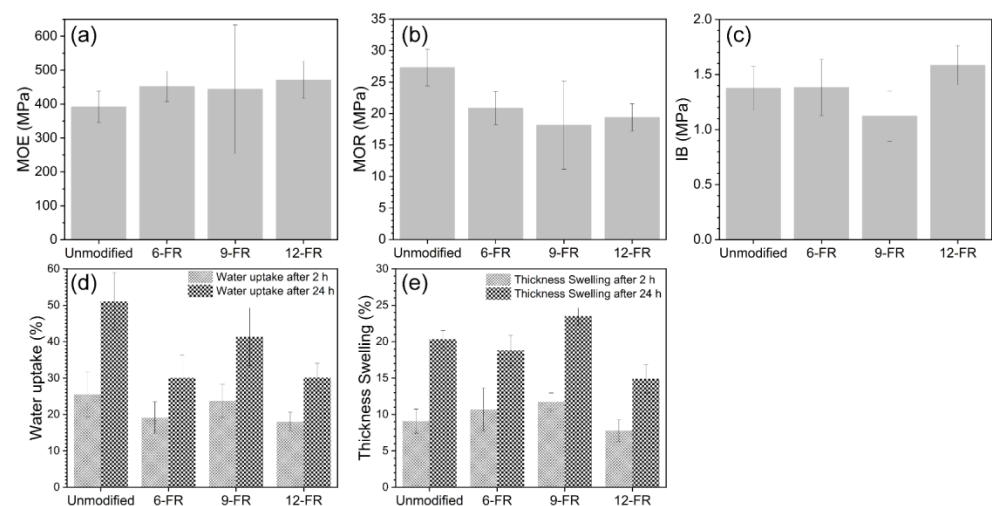


Figure 6. Mechanical and physical properties of the composite: (a) modulus of elasticity (MOE), (b) modulus of rupture (MOR), (c) internal bond strength (IB), (d) 2 h and 24 h water uptake, and (e) 2 h and 24 h thickness swelling.

The results of IB strength and water uptake/thickness swelling after 2 h and 24 h are presented in Figure 6c–e. The IB is a fundamental indicator of the adhesive bonding in wood panels [4]. The average IB for all testing specimens was estimated to be about 1.3 MPa–1.6 MPa. The addition of FRs did not have any considerable impact on the IB strength.

The thickness swelling test was conducted to evaluate the specimen's tolerance in a humid environment. The results showed that the unmodified wood composite had a water uptake of about 50% and a thickness swelling of about 20% after 24 h of water soaking. Uncommonly, the incorporation of FRs reduced the water uptake, while the extent of thickness swelling in the water was maintained; this result is positive. It should be noted that conventional ammonium phosphate salt-based retardants generally deteriorate the mechanical properties, e.g., inferior IB and thickness swelling. This is because the bonding between the wood particles and the adhesive is partially replaced by salt, and the acidic ammonium phosphate salt affects the adhesive polymerisation [4,51]. Finally, the results show a negligible influence on the mechanical properties of FR-treated composites and a slight improvement in reducing the water uptake. This is likely due to the reinforcement of the wood composite with the polymeric network of silica gel, as well as with the voids filled by the silica gel [20].

4. Conclusions

The research study demonstrated that the combination of phytic acid and sodium silicate can effectively enhance the fire retardancy of a wood composite (e.g., particleboard), while maintaining its mechanical properties. An FTIR analysis showed changes in the chemical functionalities due to the thermal degradation of hemicelluloses and the integration of phytic acid and sodium silicate into the wood. The thermal degradation resulted in a browner appearance. A SEM-EDX analysis revealed a uniform solution spraying of MUF adhesive, phytic acid, and sodium silicate, while the formation of the SiO₂ gel caused the segregation of elemental Si signals. LOI and cone calorimeter tests showed the upgraded fire resistance of the produced FR-treated wood composite resulting from the higher LOI value, the reduced heat release, the suppressed smoke production, and the increased char residue. The introduction of 12% FR additives significantly improved the overall fire-retardant properties of wood composites by reducing the release of both heat and smoke and simultaneously increasing the time to flashover. This feature of the investigated FR is exceptional, because most other FRs reduce HRR, but also concurrently increase smoke production. The TGA exhibited a lowered main decomposition temperature and increased char residue. The mechanical and physical properties of the modified composite were examined through a four-point bending test, an internal bond strength test, and thickness swelling tests, which indicated a negligible alteration in the mechanical properties, while the moisture properties were slightly improved. To conclude, this promising approach should be investigated further at the pilot-scale level, as it presents a prospective approach for the FR treatment of wood-based composites, which could increase the fire safety of the construction materials.

Author Contributions: Conceptualization, C.-F.L.; methodology, C.-F.L. and C.Z.; validation, C.-F.L., C.Z., O.K., J.M. and P.R.; formal analysis, C.-F.L. and C.Z.; investigation, C.-F.L., C.Z., J.M. and P.R.; resources, O.K. and D.S.; data curation, C.-F.L. and C.Z.; writing—original draft preparation, C.-F.L. and G.I.M.; writing—review and editing, G.I.M., O.K., J.M., P.R., D.J. and D.S.; visualization, C.-F.L.; supervision, O.K.; project administration, O.K.; funding acquisition, O.K. and D.S. All authors have read and agreed to the published version of the manuscript.

Funding: This work was supported by the Slovak Research and Development Agency under the contract No. APVV-16-0223. This work was also supported by the VEGA agency under contract No. VEGA 1/0678/22 and by the KEGA agency under the contract No. KEGA 016STU-4/2021. Support through the project “Advanced research supporting the forestry and wood-processing sector’s adaptation to global change and the 4th industrial revolution”, OP RDE (Grant No. CZ.02.1.01/0.0/0.0/16_019/000803), CT WOOD—a centre of excellence at Luleå University of Technology supported by the Swedish wood industry, and from the Swedish Research Council for Environment, Agricultural Sciences and Spatial Planning (FORMAS) project “Biobased fire protection of wood panel for exterior conditions by using phosphorylated lignin from wheat straw 2021-00818” are gratefully acknowledged herein.

Data Availability Statement: The data presented in this study are available on request from the corresponding author C.-F.L.

Conflicts of Interest: The authors declare that they have no conflict of interest.

References

1. FAO Global Forest Sector Outlook. 2050: Assessing future demand and sources of timber for a sustainable economy. *For. Work. Pap.* **2022**, *31*, 132. [[CrossRef](#)]
2. Ormondroyd, G.A. Adhesives for Wood Composites. In *Wood Composites*; Elsevier Ltd.: Amsterdam, The Netherlands, 2015; pp. 47–66, ISBN 9781782424772.
3. Östman, B.A.L.; Mikkola, E. European classes for the reaction to fire performance of wood products. *Holz Als Roh Und Werkst* **2006**, *64*, 327–337. [[CrossRef](#)]
4. Mantanis, G.I.; Martinka, J.; Lykidis, C.; Ševčík, L. Technological properties and fire performance of medium density fibreboard (MDF) treated with selected polyphosphate-based fire retardants. *Wood Mater. Sci. Eng.* **2020**, *15*, 303–311. [[CrossRef](#)]
5. Martinka, J.; Mantanis, G.I.; Lykidis, C.; Antov, P.; Rantuch, P. The effect of partial substitution of polyphosphates by aluminium hydroxide and borates on the technological and fire properties of medium density fibreboard. *Wood Mater. Sci. Eng.* **2021**, *17*, 720–726. [[CrossRef](#)]
6. Yuan, H.B.; Tang, R.C.; Yu, C.B. Flame retardant functionalization of microcrystalline cellulose by phosphorylation reaction with phytic acid. *Int. J. Mol. Sci.* **2021**, *22*, 9631. [[CrossRef](#)]
7. Sykam, K.; Försth, M.; Sas, G.; Restás, Á.; Das, O. Phytic acid: A bio-based flame retardant for cotton and wool fabrics. *Ind. Crops Prod.* **2021**, *164*, 113349. [[CrossRef](#)]
8. Patra, A.; Kjellin, S.; Larsson, A.C. Phytic acid-based flame retardants for cotton. *Green Mater.* **2019**, *8*, 123–130. [[CrossRef](#)]
9. Mokhena, T.C.; Sadiku, E.R.; Ray, S.S.; Mochane, M.J.; Matabola, K.P.; Motloung, M. Flame retardancy efficacy of phytic acid: An overview. *J. Appl. Polym. Sci.* **2022**, *139*, e52495. [[CrossRef](#)]
10. Costes, L.; Laoutid, F.; Brohez, S.; Delvosalle, C.; Dubois, P. Phytic acid–lignin combination: A simple and efficient route for enhancing thermal and flame retardant properties of polylactide. *Eur. Polym. J.* **2017**, *94*, 270–285. [[CrossRef](#)]
11. Feng, Y.; Zhou, Y.; Li, D.; He, S.; Zhang, F.; Zhang, G. A plant-based reactive ammonium phytate for use as a flame-retardant for cotton fabric. *Carbohydr. Polym.* **2017**, *175*, 636–644. [[CrossRef](#)]
12. Liu, X.H.; Zhang, Q.Y.; Cheng, B.W.; Ren, Y.L.; Zhang, Y.G.; Ding, C. Durable flame retardant cellulosic fibers modified with novel, facile and efficient phytic acid-based finishing agent. *Cellulose* **2018**, *25*, 799–811. [[CrossRef](#)]
13. Zhu, X.; Wu, Y.; Tian, C.; Qing, Y.; Yao, C. Synergistic effect of nanosilica aerogel with phosphorus flame retardants on improving flame retardancy and leaching resistance of wood. *J. Nanomater.* **2014**, *2014*, 7. [[CrossRef](#)]
14. Yan, L.; Xu, Z.; Wang, X. Synergistic flame-retardant and smoke suppression effects of zinc borate in transparent intumescent fire-retardant coatings applied on wood substrates. *J. Therm. Anal. Calorim.* **2019**, *136*, 1563–1574. [[CrossRef](#)]
15. Chen, Z.; Zhang, S.; Ding, M.; Wang, M.; Xu, X. Construction of a phytic acid–silica system in wood for highly efficient flame retardancy and smoke suppression. *Materials* **2021**, *14*, 4164. [[CrossRef](#)]
16. Schlomach, J.; Kind, M. Investigations on the semi-batch precipitation of silica. *J. Colloid Interface Sci.* **2004**, *277*, 316–326. [[CrossRef](#)] [[PubMed](#)]
17. Niu, M.; Hagman, O.; Wang, X.A.; Xie, Y.; Karlsson, O.; Cai, L.L. Effect of Si–Al Compounds on Fire Properties of Ultra-low Density Fiberboard. *BioResources* **2014**, *9*, 2415–2430. [[CrossRef](#)]
18. Katouezadeh, E.; Rasouli, M.; Zebarjad, S.M. A comprehensive study on the gelation process of silica gels from sodium silicate. *J. Mater. Res. Technol.* **2020**, *9*, 10157–10165. [[CrossRef](#)]
19. Furuno, T.; Uehara, T.; Jodai, S. Combinations of wood and silicate, III. Some properties of wood–mineral composites using the water glass–boron compound system. *Mokuzai Gakkaishi* **1993**, *39*, 561–570.
20. Garskaite, E.; Karlsson, O.; Stankeviciute, Z.; Kareiva, A.; Jonesa, D.; Sandberg, D. Surface hardness and flammability of Na₂SiO₃ and nano-TiO₂ reinforced wood composites. *RSC Adv.* **2019**, *9*, 27973–27986. [[CrossRef](#)]
21. Mai, C.; Militz, H. Modification of wood with silicon compounds. Inorganic silicon compounds and sol-gel systems: A review. *Wood Sci. Technol.* **2004**, *37*, 339–348. [[CrossRef](#)]
22. Pereyra, A.M.; Giudice, C.A. Flame-retardant impregnants for woods based on alkaline silicates. *Fire Saf. J.* **2009**, *44*, 497–503. [[CrossRef](#)]
23. ISO 4589-2:2017; Plastics—Determination of Burning Behaviour by Oxygen Index—Part 2: Ambient-Temperature Test. ISO: Geneva, Switzerland, 2017.
24. ISO 5660-1:2015; Reaction-to-Fire Tests—Heat Release, Smoke Production and Mass Loss Rate—Part 1: Heat Release Rate (Cone Calorimeter Method) and Smoke Production Rate (Dynamic Measurement). ISO: Geneva, Switzerland, 2015.
25. EN 408:2012; Timber Structures—Structural Timber and Glued Laminated Timber—Determination of Some Physical and Mechanical Properties. European Committee for Standardisation: Brussels, Belgium, 2012.
26. CEN 1993:SS-EN 319:1993; Particleboards and Fibreboards—Determination of Tensile Strength Perpendicular to the Plane of the Board. European Committee for Standardisation: Brussels, Belgium, 1993.

27. CEN 1993:BS-EN 317:1993; Particleboards and Fibreboards—Determination of Swelling in Thickness after Immersion in Water. European Committee for Standardisation: Brussels, Belgium, 1993.
28. Lin, C.; Karlsson, O.; Martinka, J.; Rantuch, P.; Garskaite, E.; Mantanis, G.I.; Jones, D.; Sandberg, D. Approaching Highly Leaching-Resistant Fire-Retardant Wood by In Situ Polymerization with Melamine Formaldehyde Resin. *ACS Omega* **2021**, *6*, 12733–12745. [[CrossRef](#)]
29. Tjeerdsma, B.F.; Militz, H. Chemical changes in hydrothermal treated wood: FTIR analysis of combined hydrothermal and dry heat-treated wood. *Holz Als Roh Und Werkst* **2005**, *63*, 102–111. [[CrossRef](#)]
30. Faix, O. Characterization in Solid State. In *Methods in Lignin Chemistry*; Lin, S.Y., Dence, C.W., Eds.; Springer: Berlin/Heidelberg, Germany, 1992; pp. 83–109.
31. Zhang, T.; Yan, H.; Shen, L.; Fang, Z.; Zhang, X.; Wang, J.; Zhang, B. Chitosan/phytic acid polyelectrolyte complex: A green and renewable intumescent flame retardant system for ethylene-vinyl acetate copolymer. *Ind. Eng. Chem. Res.* **2014**, *53*, 19199–19207. [[CrossRef](#)]
32. Li, P.; Zhang, Y.; Zuo, Y.; Lu, J.; Yuan, G.; Wu, Y. Preparation and characterization of sodium silicate impregnated Chinese fir wood with high strength, water resistance, flame retardant and smoke suppression. *J. Mater. Res. Technol.* **2020**, *9*, 1043–1053. [[CrossRef](#)]
33. Zhang, X.; Song, S.; Li, X.; Zhu, Y.; Li, X.; Xu, K.; Lyu, J.; Wu, Y. Effect of low molecular weight melamine-urea-formaldehyde resin impregnation on poplar wood pore size distribution and water sorption. *Ind. Crops Prod.* **2022**, *188*, 115700. [[CrossRef](#)]
34. Rowell, R.M.; Dienerberger, M.A. Thermal Properties, Combustion, and Fire Retardancy of Wood. In *Handbook of Wood Chemistry and Wood Composites*; Rowell, R.M., Ed.; CRC Press: Boca Raton, FL, USA, 2013; pp. 127–149, ISBN 9781439853818.
35. Fengel, D.; Wegener, G. Influence of Temperature. In *Wood Chemistry, Ultrastructure, Reactions*; Walter de Gruyter: Berlin, Germany; New York, NY, USA, 1989; pp. 319–344.
36. Devallencourt, C.; Saiter, J.M.; Fafet, A.; Ubrich, E. Thermogravimetry/Fourier transform infrared coupling investigations to study the thermal stability of melamine formaldehyde resin. *Thermochim. Acta* **1995**, *259*, 143–151. [[CrossRef](#)]
37. Chen, J.P.; Isa, K. Thermal Decomposition of Urea and Urea Derivatives by Simultaneous TG/(DTA)/MS. *J. Mass Spectrom. Soc. Jpn.* **1998**, *46*, 299–303. [[CrossRef](#)]
38. Ullah, S.; Bustam, M.A.; Nadeem, M.; Naz, M.Y.; Tan, W.L.; Shariff, A.M. Synthesis and thermal degradation studies of melamine formaldehyde resins. *Sci. World J.* **2014**, *2014*, 940502. [[CrossRef](#)] [[PubMed](#)]
39. LeVan, S.L. Chemistry of fire retardancy. In *The Chemistry of Solid Wood*; Rowell, R., Ed.; American Chemical Society: Washington, DC, USA, 1984; pp. 531–574.
40. Bahari, A.; Ghovati, M.; Hashemi, A. Studying of SiO₂/capron nanocomposite as a gate dielectric film for improved threshold voltage. *Appl. Phys. A Mater. Sci. Process.* **2019**, *125*, 1–7. [[CrossRef](#)]
41. Ritchie, S.J.; Steckler, K.D.; Hamins, A.; Cleary, T.G.; Yang, J.C.; Kashiwagi, T. The Effect of Sample Size on the Heat Release Rate of Charring Materials. In Proceedings of the Fire Safety Science—Proceedings of the 5th International Symposium; Hasemi, Y., Ed.; International Association for Fire Safety Science: Melbourne, Australia, 1997; pp. 177–188.
42. Martinka, J.; Hroncová, E.; Chrebet, T.; Balog, K. The influence of spruce wood heat treatment on its thermal stability and burning process. *Eur. J. Wood Wood Prod.* **2014**, *72*, 477–486. [[CrossRef](#)]
43. Lin, C.F.; Karlsson, O.; Das, O.; Mensah, R.A.; Mantanis, G.I.; Jones, D.; Antzutkin, O.N.; Försth, M.; Sandberg, D. High Leach-Resistant Fire-Retardant Modified Pine Wood (*Pinus sylvestris* L.) by In Situ Phosphorylation and Carbamylation. *ACS Omega* **2023**, *8*, 11381–11396. [[CrossRef](#)] [[PubMed](#)]
44. Zhang, S.; Wang, X.; Ding, M.; Huang, Y.; Li, L.; Wang, M. In-situ incorporation of metal phytates for green and highly efficient flame-retardant wood with excellent smoke-suppression property. *Ind. Crops Prod.* **2022**, *187*, 115287. [[CrossRef](#)]
45. Nagaoka, T.; Tsujimoto, M.; Kodaira, A.; Uehara, S.; Kikuchi, S. Relationship Between Density and Ignition Time of Wooden Materials. *J. Struct. Constr. Eng.* **2002**, *67*, 233–236. [[CrossRef](#)]
46. SS-EN 45545-2:2021; Railway Applications—Fire Protection on Railway Vehicles—Part 2: Requirements for Fire Behaviour of Materials and Components. European Committee for Standardisation: Brussels, Belgium, 2021.
47. Marquis, D.; Guillaume, E.; Lesenechal, D. Accuracy (trueness and precision) of cone calorimeter tests with and without a vitiated air enclosure. *Procedia Eng.* **2013**, *62*, 103–119. [[CrossRef](#)]
48. ISO 9705-1:2017; Reaction to Fire Tests—Room Corner Test for Wall and Ceiling Lining Products—Part 1: Test Method for a Small Room Configuration. ISO: Geneva, Switzerland, 2017.
49. Östman, B.A.; Tsantaridis, L.D. Correlation between cone calorimeter data and time to flashover in the room fire test. *Fire Mater.* **1994**, *18*, 205–209. [[CrossRef](#)]
50. Xu, J.; Zhang, Y.; Shen, Y.; Li, C.; Wang, Y.; Ma, Z.; Sun, W. New perspective on wood thermal modification: Relevance between the evolution of chemical structure and physical-mechanical properties, and online analysis of release of VOCs. *Polymers* **2019**, *11*, 1145. [[CrossRef](#)]
51. Ayrilmis, N. Effect of fire retardants on internal bond strength and bond durability of structural fiberboard. *Build. Environ.* **2007**, *42*, 1200–1206. [[CrossRef](#)]

Disclaimer/Publisher’s Note: The statements, opinions and data contained in all publications are solely those of the individual author(s) and contributor(s) and not of MDPI and/or the editor(s). MDPI and/or the editor(s) disclaim responsibility for any injury to people or property resulting from any ideas, methods, instructions or products referred to in the content.